The tautomeric equilibrium and stereochemistry of β-sulfonyl enamines†

Lech Kozerski,*[ab] Brunon Kwiecień,[a] Piotr Krajewski,[a] Robert Kawęcki,[a] Elżbieta Bednarek,[b] Jerzy Sitkowski,[ab] Wojciech Bocian,[b] Wiktor Koźmiński[c] and Poul Erik Hansen[d]

[a] *Institute of Organic Chemistry, Polish Academy of Sciences, Kasprzaka 44, 01-224, Warsaw, Poland. E-mail: lkoz@icho.edu.pl; Fax: +48 (22) 632 66 81; Tel: +48 (22) 632 3221 2018*
[b] *Drug Institute, Chelmska 30/34, 00-725, Warsaw, Poland*
[c] *Department of Chemistry, Warsaw University, Pasteura 1, 02-093, Warsaw, Poland*
[d] *Department of Life Sciences and Chemistry, Roskilde University, 4000, Roskilde, Denmark*

Received* (*in Montpellier, France*) *7th January 2002, Accepted 6th March 2002
First published as an Advance Article on the web 3rd July 2002

Compounds of three groups of parent secondary aliphatic β-sulfonyl enamines, unsubstituted or with an alkyl substituent in the α or β positions, have been studied. The β-sulfonyl enamines are found in equilibria between the E and Z enamine and imine forms in varying amounts in $CDCl_3$ solution. ^1H, ^{13}C and ^{15}N data were acquired and used for the assignment of the three species in solution. Considerable variations in the amounts of enamine E and Z and imine forms are found, depending on the substitution pattern. The conformational space of the equilibrated tautomers have been investigated using steady-state NOE experiments, dynamic NMR and $^nJ(H,H)$ and $^nJ(C,H)$ long-range spin-spin coupling constants, as well as *ab initio* HF and DFT calculations for structure determination and relative energy evaluations. Based on NOE, saturation transfer experiments and conformational analysis, an equilibrium scheme is proposed showing the mechanism and the involvement of water in the transformation of β-sulfonyl imines into the corresponding enamines.

β-Sulfonyl enamines (β denotes that the sulfonyl group is at C^2 with respect to the amine group, see Scheme 1) may be considered as vinyl analogues of sulfonamides, an important class of compounds due to their biological activity.[1] At the same time, they belong to the wide class of "push-pull" ethylenes. The sulfone group plays an important role in organic synthesis. Due to its strong σ-electron withdrawing properties,[2,3] it is commonly introduced in an α-position as an activator to enhance the acidity of protons. Furthermore, the σ-electron effect is in contrast to that in enaminones or enamino lactones in which the carbonyl group also participates in π-electron conjugation. Due to the aforementioned electronic properties, β-sulfonyl enamines are unique as three tautomeric forms, namely Z and E enamines and imine (I), are present in equilibrium in $CDCl_3$ solution for most of the compounds studied here (Scheme 1). In contrast, for the β-sulfinyl enamines only the enamine E form and imines were observed with few exceptions such as in ref. 4, where the Z enamine was also observed.

Tautomerism is one of the fundamental physical processes that underlies many important chemical transformations and in particular, keto-enol equilibria are frequently studied.[5,6] Despite the importance of the imine-enamine tautomerism in bioorganic and heterocyclic chemistry, only scarce data exists from both theoretical and experimental points-of-view. The last decade has yielded unprecedented progress in theory and development of computational facilities, both of which have prompted renewed interest in this problem.[7–10]

The classic experimental work of McMullen and Stirling cites several examples of equilibria in aliphatic β-sulfonyl enamines.[11] However, no systematic attempts to study the interrelations between the substituent steric or electronic character and the tautomeric composition were presented before the present work. A recent review on tautomerism involving nitrogen and oxygen[12] cites examples of the equilibrium in aromatic β-sulfonyl enamines.[13] The energy difference between enamine and imine in simple compounds is very small and is overshadowed by solvent effects. The mechanistic investigations so far are restricted to a theoretical calculation of a 1,3-sigmatropic proton transfer.[7]

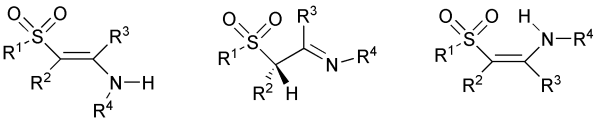

E-Z **I-E** **Z-E**

	R^1	R^2	R^3	R^4
1	Me	H	H	Me
2	Me	H	H	Et
3	Me	H	H	*i*-Pr
4	Me	H	H	*t*-Bu
6	Et	Me	H	*t*-Bu
7		$-(CH_2)_3-$	H	*t*-Bu
8	Me	H	Me	*i*-Pr
9	Me	H	Me	*t*-Bu

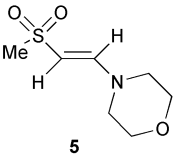

5

Scheme 1

† Electronic supplementary information (ESI) available: NMR spectra and tables of NMR data. See http://www.rsc.org/suppdata/nj/b2/b200205a/

 DOI: 10.1039/b200205a

The simultaneous presence of the three tautomeric forms in the slow-exchange regime on the NMR timescale offered, for the first time in activated enamines, a unique opportunity to study the steric and electronic factors affecting the populations. In particular, we were interested in uncovering the intramolecular and solvent conditions that would promote the imine form, which is potentially of high synthetic utility. This was a leading motivation to undertake the study. This is because of the recent expressed interest by synthetic chemists in the azomethine functionality, due to its use in enantioselective catalytic addition, reductive amination or carbon–carbon bond formation.[14] Denmark and Nicaise have also shown that enolisable imines are good substrates in enantioselective alkylations by alkali metals activated by chiral auxiliaries.[15]

Furthermore, as the cited contributions indicate, there has been no systematic study of the stereochemistry and intramolecular dynamics or of the tautomeric equilibrium in the parent aliphatic compounds studied here. In view of the rare and accidental studies of these phenomena this work seems to be the first systematic study of the above topics, which have a general application to enamine chemistry. In particular, in order to fill the gap in understanding the proton transfer mechanism of enamine-imine tautomerism, we have investigated NOE and saturation transfer in β-sulfonyl enamines and studied the conditions influencing the above equilibrium in various solvents.

Results

General considerations

The compounds studied in this work are represented by the general formula shown in Scheme 1 and exist in solution in a tautomeric equilibrium. The isomers in equilibrium are named with respect to the stereochemistry along the C^2=C^1 bond and C^1–N bonds, namely E–Z isomerism around the formal double C^1=C^2 bond and hindered rotation around the C^1–N bond, which for some of the compounds is slow at low temperatures on the NMR timescale.

The interconversion of tautomers is in the slow-exchange regime on the NMR chemical shift timescale at 200 or 500 MHz. A representative spectrum is given for compound **8** recorded at −60 °C at 500 MHz, showing three sets of resonances for the corresponding tautomeric forms at equilibrium [Fig. 1S; see Electronic supplementary information (ESI)]. This demonstrates primarily the fact that no spectral changes are observed on cooling the sample from ambient temperature. This observation shows that rotations around the S–C^2, C^1–N and N–C^N bonds are essentially either fixed or free. The lack of temperature dependence of the ^3J(N**H**,C^1**H**) coupling constant suggests the predominance of a single conformation around the N–C^N bond. In contrast to **8**, the DNMR study of **1**–**4**, performed at temperatures down to −50 °C, evidences different conformational species compared to those present at ambient temperature (see Table 1). In the case of C^2-methyl-substituted compounds the TOCSY spectrum, shown in Fig. 2S (see ESI) for **7**, allows unambiguous assignment of the signals.

In Table 1S (see ESI) the ^{1}H T_1 relaxation times data are given for compound **8**, which was chosen for a detailed NOE study and saturation transfer experiments. The ^{1}H T_1 relaxation times for signals of the three tautomeric species in solution are given in Table 1S.

The assignments of ^{1}H resonances are accomplished using established earlier structural dependencies of NMR parameters in enamines.[16,17] The values observed for δ NH in imines agree with the values usually found for this type of nitrogen atom.[18]

Scheme 2 summarises the types of conformations in the compounds discussed in the text.

Measurement and assignment of long-range coupling constants

The following types of coupling constants are of interest in the present structural studies: ^3J(**H**^{1}, N**H**), ^3J(**C**^{2}, N**H**), ^3J(N**H**, C^N**H**), ^3J(**C**^{1}, C^N**H**) and finally ^3J(C^1–**C**H_3, N**H**) for the derivatives with a methyl substituent at the C^1 carbon atom. For the determination of ^nJ(C,H) coupling constants a HSQC version of the HECADE approach was used.[19] A detailed description of the experiments and the results are presented in a recent paper for this class of compounds.[20]

The stereochemical assignments using vicinal proton-proton spin-spin coupling constants are based on application of the theoretical coupling constants as obtained from the Osawa equation.[21] The ^3J(H,H) values are cited in Table 1 and some available ^3J(C,H) coupling constants are given in Table 2S (see ESI).

Calculations

Structures and the corresponding energies have been calculated at three different levels of theory in order to provide the necessary internuclear distances for NOE simulations. The results are presented in Tables 2, 3 and 4.

The MMX PCMODEL approach has been used previously.[22,23] The *ab initio* methods and the density functional theory (DFT) approach are also introduced. The resulting geometries obtained by these methods for **8** may be compared to the solid state structure as determined by X-ray diffraction (see Table 4).[24] The energies in Table 2 show that the imine form has the lowest energy for **7** and almost the lowest energy for **3** and **9**. Not unexpectedly, this picture does not fully reflect the experimental findings as also seen in Table 2. This can most likely be related to the fact that the energy differences are small and also that solvent effects are not taken into account in the calculations.

NOE data

To gain information concerning the tautomeric exchange mechanism, both water non-exchangeable (Table 5) and exchangeable (Table 6) protons were irradiated in saturation transfer experiments. The steady-state saturation transfer experimental data for **8** show that irradiation of the water signal gives saturation transfer to the Z-NH, E-NH and C^2H_2 imine signals, evidencing intermolecular exchange of water with the three species in solution (Table 6). The above observations concerning exchange between tautomeric forms find support in the ROESY exchange cross-peaks and negative 1D ^{1}H NOE values of **8** in $CDCl_3$ at +30 °C on a degassed sample. The important corresponding negative 1D NOE values are summarised in Scheme 3 and Table 5.

A saturation transfer experiment conducted on compound **7** showed that no transfer from either NH or C^2H of imine to water nor from water to these resonances takes place. On the other hand, an experiment performed with compound **4** (see Table 5S in ESI) shows the transfer from imine to water and the acquired information is, in general, similar to that found for **8** at a similar concentration.

Discussion

The relative populations of the two enamine forms Z and E can be interpreted as an interplay of two counterbalancing factors: (*i*) the strength of H-bond favouring the Z form and (*ii*) steric compression. Steric compression may cause further stabilisation of the Z form as seen in a comparison of the concentrations of this form in **4** and **9** *vs.* **7**. The steric compression of two bulky groups (R^3 and R^4) results in a markedly decreased O···H–N distance (Table 2), leading to a stronger

Table 1 ^{1}H NMR chemical shifts and spin-spin coupling constants ^{n}J in β-sulfonyl enamines of the type R^1–SO_2–C^2R^2=C^1R^3–NHR^4 in $CDCl_3$ solution at 27 °C (R^1–R^4 are given in Scheme 1). For some compounds ^{15}N NMR data are also included.[a]

	Isomer (%)	Chemical shift/ppm and ^{n}J/Hz				
		R^1	R^2	R^3	R^4	NH [δ^{15}N]
1	E–Z + E–E (97)[b]	2.89	4.98 $^{3}J(H^1,H^2) = 12.8$	7.30 $^{3}J(H^1,H^2) = 12.8$ $^{3}J(H^1,NH) = \mathbf{7.4}$	2.69 $^{3}J(NH,CH_3) = 6.0$	4.80 [−305.2]
	Z (3)		4.55 $^{3}J(H^1,H^2) = 8.1$	6.50 $^{3}J(H^1,H^2) = 8.1$		6.55
2	E–Z + E–E (84)	2.93	5.08 $^{3}J(H^1,H^2) = 12.8$	7.30 $^{3}J(H^1,H^2) = 12.8$ $^{3}J(H^1,NH) = \mathbf{8.0}$	1.21, 3.05 ^{3}J (NH,CH_2) = 8.0	4.75
	Z (13)		4.54 $^{3}J(H^1,H^2) = 8.4$	6.58 $^{3}J(H^1,H^2) = 8.4$ $^{3}J(H^1,NH) = 13.8$		6.74
3	E–Z + E–E (87)	2.92	5.06 $^{3}J(H^1,H^2) = 12.9$	7.22 $^{3}J(H^1,H^2) = 12.9$ $^{3}J(H^1,NH) = \mathbf{9.1}$	3.37, 1.18	4.77 [−275.9]
	Z (10)	2.94	4.56 $^{3}J(H^1,H^2) = 8.2$	6.58 $^{3}J(H^1,H^2) = 8.2$ $^{3}J(H^1,NH) = 7.68$[c]	3.34, 1.18	6.64 [−274.8]
	I (3)	2.90	3.88 $^{3}J(H^1,CH_2) = 5.3$		–[c], 1.15	– [−12.0]
	E–E (30)[d]	–[c]	5.17 $^{3}J(H^1,H^2) = 12.5$	7.13 $^{3}J(H^1,H^2) = 12.5$	–[c]	5.13 $^{3}J(H^1,NH) = 12.0$
	E–Z (57)[d]	2.94	4.98 $^{3}J(H^1,H^2) = 13.0$	7.20 $^{3}J(H^1,H^2) = 13.0$	3.34, 1.15	4.95 $^{3}J(H^1,NH) = 7.5$
	Z (12)[d]	2.94	4.52 $^{3}J(H^1,H^2) = 8.0$	6.60[b]	3.34, 1.15	6.60
	I (1)[d]	–[c]	4.1	7.78	–[c]	[–]
4	E (60)	2.94	5.17 $^{3}J(H^1,H^2) = 13.0$	7.29 $^{3}J(H^1,H^2) = 13.0$ $^{3}J(H^1,NH) = \mathbf{14.0}$	1.29	4.69 $^{3}J(H^1,NH) = 14.0$ [−269.6]
	Z (32)	2.95	4.61 $^{3}J(H^1,H^2) = 8.5$	6.69 $^{3}J(H^1,H^2) = 8.5$ $^{3}J(H^1,NH) = 14.5$	1.26	6.93 $^{3}J(H^1,NH) = 14.5$ [−266.8]
	I (8)	2.89	3.93 $^{3}J(H^1,CH_2) = 5.5$	7.73 $^{3}J(H^1,CH_2) = 5.5$	1.24	[−4.7]
5	E (100)	2.88	4.99 $^{3}J(H^1,H^2) = 12.8$	7.11 $^{3}J(H^1,H^2) = 12.8$	3.15 (N–CH_2), 3.65 (O–CH_2)	[−291.0]
6	E (93)	1.21, 2.89 $^{3}J = 7.5$	1.71	7.23 $^{3}J(H^1,NH) = 14.2$ $^{4}J(H^1,CH_3) = 0.9$	1.27	4.11 $^{3}J(H^1,NH) = 14.2$ [−273.8]
	Z (7)	1.39, 2.98	1.83 $^{4}J(H^1,CH_3) = 0.5$	6.56 $^{3}J(H^1,NH) = 13.5$ $^{4}J(H^1,CH_3) = 0.5$	1.27	6.07 $^{3}J(H^1,NH) = 13.5$ [−273.8]
7	E (58)	–[e]		6.98 $^{3}J(H^1,NH) = 14.0$	1.24	3.88 $^{3}J(H^1,NH) = 14.0$ [−276.0]
	Z (21)			6.43 $^{3}J(H^1,NH) = 13.5$	1.21	5.36 $^{3}J(H^1,NH) = 13.5$ [−277.6]
	I (21)[f]			7.63 $^{3}J(H^1,CH_2) = 5.0$		[−12.9]
8	Z (20)	2.84	4.40	1.86	1.12, 3.65	3.98 [−267.8]
	E (65)	2.90	4.84	2.14	1.11, 3.45	6.95 [−271.8]
	I (15)	2.87	3.78	2.01	1.07, 3.74	[−27.5]
9	Z (46)	2.90	4.44	2.03	1.35	4.10
	E (54)	2.96	5.07	2.18	1.33	7.30

[a] Twenty-five milligrams of a solute was dissolved in 0.7 mL $CDCl_3$ and the solution was allowed to equilibrate overnight, unless otherwise indicated. [b] Measured directly after dissolving the compound. [c] Not determined. [d] Taken at −20 °C for the same sample of the **3**, as used for the 27 °C measurements. [e] Proton assignments shown in the legend to TOCSY spectrum in Fig. 2S. [f] Population of the imine may rise to 60% in benzene solution.

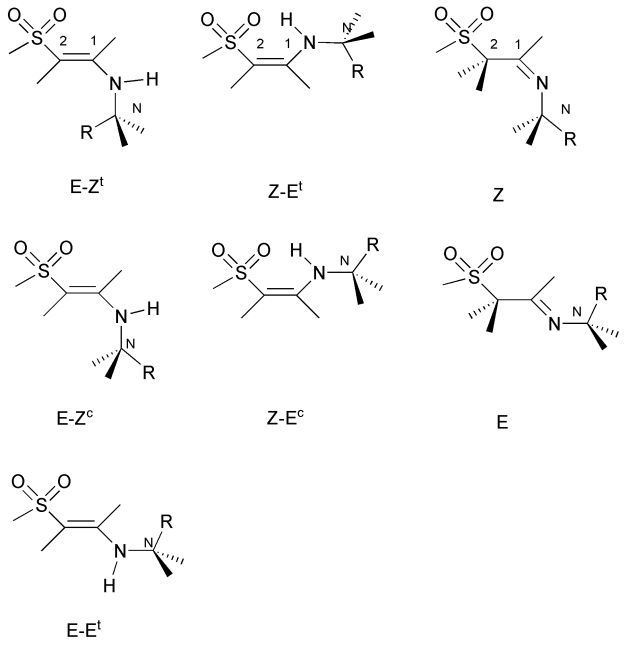

Scheme 2 Conformational isomers. R can denote both H and CH_3. The descriptor in capitals denotes the configuration and conformation along the C^2=C^1 and C^1–N bonds, respectively. The superscript denotes the conformation along the N–C^N bond, taking into account that the R is in the plane of the NH proton.

hydrogen bond as reflected by the value of the NH chemical shifts (Table 1).

Tautomeric and conformational equilibria

The data gathered in Table 1 allow several conclusions with regard to features influencing the tautomeric equilibrium. Firstly, it is seen that compounds unsubstituted on the double bond, **1**–**5**, form predominantly E species (although in this context **5** is not relevant because it is tertiary and only has the E form and cannot be 'predominantly'). For compound **1** this is almost the only form detected. The E form is also predominant for the C^2-substituted compounds, **6** and **7**, but the Z form is the major tautomer for the C^1-substituted derivatives, **8** and **9**.

Because tautomerisation processes in the present case may be strongly dependent on stereochemical features, a detailed study of conformational space was undertaken using *ab initio* and molecular modelling methods and experimental NMR techniques: steady-state NOE, classic DNMR and measurement of long-range coupling constants, ^nJ(C,H), to characterise preferred conformations around the C^2=C^1, S–C^2, C^1–N and N–C^N bonds.

The distinction between E and Z isomers of the C^2=C^1 bond is straightforward using vicinal H,H coupling constants. In the absence of the above coupling constant the δ NH values can be used with the following characteristics: E isomer (3.9–4.2 ppm) and Z isomer (6.5–7.5 ppm)[16] in $CDCl_3$ solutions. The rotation around the double bond is in the slow-exchange regime and sharp resonances are observed. Furthermore, no exchange cross-peaks are observed in the ROESY spectra between the two forms.

The rotation around the S–C^2 bond is essentially free and our molecular mechanics data show that the dihedral angle CH_3–S–C^2=C^1 in **8** may have values around ±180° or ±60–80° (*vide infra*). From the value of ^3J (**C**H_3–S, C^2**H**), *ca.* 0 Hz for all compounds, the latter alternative seems the most likely as also confirmed by the X-ray structure (seeTable 4).[24]

The detailed insight into the stereochemistry of the E form generated by the C^1–N degree of freedom is obtained by the vicinal ^3J(C^1**H**, N**H**) coupling constants in the unsubstituted compounds, **1**–**4**, or C^2-alkyl-substituted derivatives, **6** and **7**. However, for the C^1-methyl-substituted compounds the methods of choice are NOE measurements or ^3J(**C**H_3, N**H**), ^3J(**C**^{2}, N**H**) and ^3J(**C**^{1},C^N**H**) coupling constant determinations. It is shown in Table 1 that the vicinal coupling constant along the C^1–N bond, ^3J(C^1**H**, N**H**), is increasing from 7.5 to 14 Hz at room temperature with increase of the bulk of the substituent at the nitrogen atom in the order CH_3 < C_2H_5 < *i*-C_3H_7 < *t*-C_4H_9. For **1** the conformation is preferentially E–Z whereas for **4** the overwhelming preference is E–E. For **3** the ^3J(C^1**H**, N**H**) coupling points to a mixture of E–Z and

Table 2 Calculated energies and dipole moments for the lowest energy conformers[a]

Comp.	Isomer	Torsion angles/° Me–S–C^2–C^1	C^2–C^1–N–C^N	H–N–C^N–R	Relative energy[b] / kcal mol^{-1}	Dipole moment/D	Exptal population (in $CDCl_3$)	Hydrogen bond length[c]/Å
3	E–E^t	111.59	−164.38	171.11	+2.5	6.94	0.30	
	E–Z^t	115.39	4.81	152.03	+2.8	7.35	0.57	
	Z–E^t	114.75	168.82	−171.02	0	6.04	0.12	2.80
	I–E[d]	73.95	179.95		+0.9	4.60	0.01	(1.97)
7	E–E^c	154.39	−164.90	34.58	+2.1	6.91		
	E–Z^c	151.39	−24.56	−11.01	+8.0		0.58	
	Z–E^c	150.26	−163.79	37.18	+0.9	5.51	0.21	2.97
	I–E[d]	−111.49	−179.81		0	4.59	0.21	(2.15)
8	E–E^t	94.44	−153.14	170.76	+5.4	7.25		
	E–Z^t	97.74	4.52	151.85	+4.2	7.59	0.20	
	Z–E^t	119.54	−166.36	167.06	−0.04	6.63	0.65	2.79
	I–E[d]	74.30	−179.88		0	4.69	0.15	(1.90)
9	E–E^c	94.23	−144.79	28.32	+5.5	7.14		
	E–Z^c	88.33	−4.86	−9.36	+3.4	7.60	0.46	
	Z–E^c	115.29	−160.01	19.67	0	6.63	0.54	2.79
	I–E[d]	75.14	179.77		+0.8	4.82	0.0	(1.88)

[a] Energies and dipole moments obtained from DFT calculations using the BLYP, 6-31G** level of theory. In the torsion H–N–C^N–R, R denotes a C^N**H** or methyl group (*t*-butyl derivative) in the N–H plane (see Scheme 2). Isomeric composition, calculated from NMR spectra, are given for **3** at −20 °C, and for **7**–**9** at 27 °C (E–E and E–Z are given together). [b] Total SCF energy, relative to the lowest energy conformer. [c] Distances between S=**O** and **H**N atoms (in parentheses) and O···N atoms in Z–E isomers. [d] The torsion angle S–C^2–C^1–N in **3**, **7**, **8**, and **9** is −97.75, 114.20, −90.78 and −89.47°, respectively. The C^1–N–C^N–R torsion (R denotes C^N**H** or methyl group coplanar with C^1=N bond) in **3**, **7**, **8** and **9** is 0.66, 1.31, 4.48 and 177.77°, respectively.

Table 3 Parameters for the low-energy conformers of **Z–8**. Conformers best fitted to the steady-state NOE date are given in bold. RMS_{NOE}[23] factors are calculated using external relaxation = 2.1 Å

No.[a]	Energy/ kcal mol^{-1}	Torsion angles/°			Conformation	RMS_{NOE}
		Me–S–C^2–C^1	C^2–C^1–N–C^N	C^1–N–C^N–H		
1	**3.21**	**76.1**	**−171.7**	**−33.0**	**Z–E^t**	**0.375**
2	**3.57**	**163.6**	**−174.4**	**−31.1**	**Z–E^t**	**0.380**
3	**3.72**	**124.0**	**170.4**	**33.8**	**Z–E^t**	**0.359**
4	**3.85**	**111.0**	**166.8**	**27.8**	**Z–E^t**	**0.382**
5	6.41	−73.6	170.9	−160.0	Z–E^c	0.800
6	6.58	−57.7	143.3	−146.4	Z–E^c	0.745
7	8.39	50.8	122.7	−158.6	Z–E^c	0.829
ab initio (**HF**)	**0**[b]	**108.3**	**−171.9**	**−28.7**	**Z–E^t**	**0.369**
ab initio (HF)	4.6[b]	101.4	162.0	−179.9	Z–E^c	0.835
DFT	–	**119.5**	**−166.4**	**−30.6**	**Z–E^t**	**0.374**

[a] MMX derived files are numbered in Arabic. Data are from a global minimum search using the multiple torsion option (MULTOR). Total energy in the force field used by the program MM3. [b] Total electronic energy, relative to the lowest energy conformer.

Table 4 Parameters for the low-energy conformers of **E–8**. Conformers best fitted to the steady-state NOE date are given in bold. RMS_{NOE}[23] factors are calculated using external relaxation = 2.2 Å

No. [a]	Energy/kcal mol^{-1}	Torsion angles/°			Conformation	RMS_{NOE}
		Me–S–C^2–C^1	C^2–C^1–N–C^N	C^1–N–C^N–H		
1	3.93	−71.2	167.2	−14.25	E–E^t	1.310
2	**4.02**	**−55.3**	**−11.1**	**−26.2**	**E–Z^t**	**0.253**
3	**4.09**	**77.0**	**12.8**	**25.3**	**E–Z^t**	**0.240**
4	**4.17**	**−175.6**	**12.5**	**25.2**	**E–Z^t**	**0.250**
5	**4.17**	**175.3**	**−15.2**	**−21.9**	**E–Z^t**	**0.248**
6	**4.19**	**−176.6**	**−10.7**	**−26.8**	**E–Z^t**	**0.252**
7	7.68	−165.4	−146.3	140.7	E–E^c	1.218
X-Ray[24]	[b]	**−76.4(2)**	**−9.7(2)**	**41.5**	**E–Z^t**	**0.251**
***ab initio* (HF)**		**92.8**	**−0.2**	**−38.1**	**E–Z^t**	**0.235**
DFT	1.2[c]	94.4	−153.1	−42.0	E–E^t	1.218
DFT	**0**[c]	**97.7**	**4.52**	**−40.8**	**E–Z^t**	**0.226**

[a] MMX derived files are numbered in Arabic. Data are from a global minimum search using the multiple torsion option (MULTOR). Total energy is in the force field used by the program MM3. [b] Geometry from X-ray, not minimised in MM field. [c] Total electronic energy, relative to the lowest energy conformer.

Table 5 Saturation transfer data for compound **8** at 30 °C

Irradiated	Observed					
	E–CH_3	Z–CH_3	I–CH_3	E–C^NH	Z–C^NH	I–C^NH
E–CH_3	*		−6.5[a]			
			−8.5[b]			
			−7.7[c]			
Z–CH_3		*	−17.0[a]			
			−25.0[b]			
			−36.0[c]			
I–CH_3	−5.0[a]	−5.0[a]	*			
	−8.7[b]	−8.0[b]				
	−6.5[c]	−12.0[c]				
E–C^NH				*		−7.2[a]
						−10.0[b]
						−7.2[c]
Z–C^NH					*	−22.0[a]
						−26.0[b]
						−40.0[c]
I–C^NH				−5.8[a]	−18.0[a]	*
				−9.7[b]	−16.0[b]	
				−8.2[c]	−20.0[c]	

[a] Ten milligram sample with initial enamine:H_2O molar ratio = 2.5:1. [b] Ten milligram sample with initial enamine:H_2O molar ratio = 1:1. [c] Two milligram sample with initial enamine:H_2O molar ratio = 1:2.

Table 6 Saturation transfer between dynamic protons at 30 °C in **8**[a]

Irradiated	Observed					
	Z–NH	E–C^2H	Z–C^2H	E–NH	I–C^2H_2	H_2O
Z–NH	*					−3.2
E–C^2H		*			−2.7	0
					(–3.4)[b]	
Z–C^2H	0.7		*		−8.6	0
					(–7.1)	
E–NH				*	−1.8	−2.9
I–C^2H_2	−0.3	−7.3	−13.4	−3.5	*	−4.6
		(–6.3)	(–10.3)			
H_2O	−8.3	0	0	−11.3	−12.0	*
	(–3.1)				(–7.8)	

[a] Ten milligram sample in 0.7 mL $CDCl_3$ at 30 °C, degassed; isomer ratio E:Z:I = 0.58:0.24:0.18; initial enamine:H_2O molar ratio = 2.5:1. [b] Values in brackets for the same sample including an additional 0.5 μL H_2O.

E–E forms (see Table 1). The detailed ^{1}H and ^{13}C DNMR studies performed on compounds **1–4** confirm the conformational equilibrium change obtained from the $^3J(C^1\mathbf{H}, N\mathbf{H})$ coupling constants.

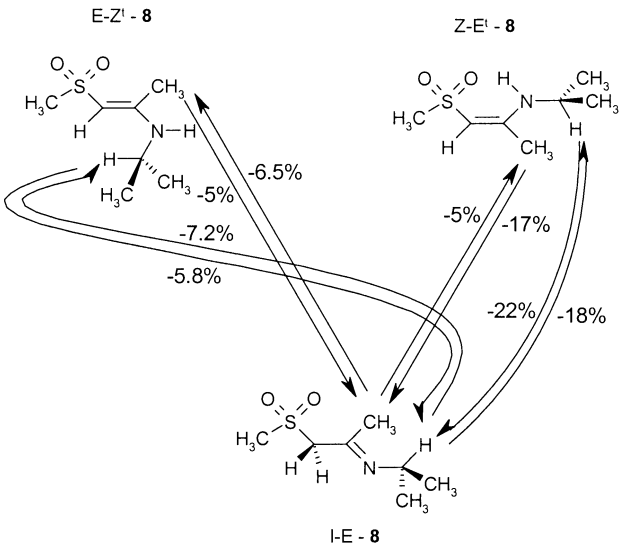

Scheme 3 Saturation transfer experiment. For details see Table 6.

C^2-alkyl-substituted compounds with *N-t*-Bu groups have a transoid conformation along the C^1–N bond as shown for **6** and **7** in Table 1, characterised by a $^3J(C^1\mathbf{H}, N\mathbf{H})$ coupling constant of 14.2 and 14.0 Hz, respectively. The DNMR study does not show any temperature variation of the spectral parameters in the environment of the C^1–N bond.

The conformational analysis using DNMR and proton-proton coupling constants is summarised as follows: the E tautomers of unsubstituted compounds of the type **1**–**4** are not conformationally homogeneous and exist in a fast equilibrium of E–Z and E–E forms, whereas the latter conformation prevails in C^2-substituted derivatives such as **6** and **7**. In the following it will be shown that C^1-methyl-substituted compounds, like **8**, exist predominately in the E–Z conformation.

The N–C^N bond. In the C^1-methyl-substituted derivative **8**, the conformational space is complicated by an additional degree of freedom, a free rotation around the N–C^N bond. This is concluded from the DNMR study (see Fig. 1S in ESI), showing no spectral process similar to those observed in **1**–**4** and no changes, for both E and Z forms, of the $^3J(N\mathbf{H}, C^N\mathbf{H})$ coupling constants, which are 7.3 and 9.0 Hz, respectively. Therefore, we have based the conformational equilibrium assignments on complementary ^{1}H NOE data and ^3J(C,H) values. While NOE effects give information on the overall averaged conformations along the C^1–N and N–C^N bonds, the ^3J(C,H) coupling constants give independent information for both degrees of freedom. The coupling constants specific for the C^1–N bond are the vicinal $^3J(\mathbf{C^2}, N\mathbf{H})$ and $^3J(C^1\mathbf{C}H_3, N\mathbf{H})$ couplings, whereas rotation around the N–C^N bond can be probed by $^3J(\mathbf{C^1}, C^N\mathbf{H})$ complemented with $^3J(N\mathbf{H}, C^N\mathbf{H})$. These data are discussed later.

The steady-state NOE's. Table 3S (see ESI) gives the experimental NOE's and Table 3 gives the results of the conformational search and a comparison of the experimental 1D ^{1}H NOE results for the Z isomer of **8** compared, by means of the RMS factor, with the theoretical ones calculated using our program for back-calculation of NOE's from MMX data.[23]

The conformation **3** in Table 3 fits best the experimental data. This conformation is of the Z–E^t type (Scheme 2) with intramolecular hydrogen bonding (torsion angle Me–S–C^2=C^1, 124°). Mixing in 20% of conformation **6** (Z–E^c) lowers the RMS to 0.299, but this change is not statistically meaningful.[23] However, it should be noticed that the RMS values are rather high. Taking this reservation into account, the mono-conformation model of the type Z–E^t is favoured, on the basis of the NOE data, and the presence of a considerable amount of the Z–E^c conformation is not likely, although such a mixture could have been expected on the basis of the $^3J(C^N\mathbf{H}, N\mathbf{H})$ value, 9.0 Hz, which is lower than the predicted value for the Z–E^t conformation, *ca.* 13 Hz[21] (see above).

Table 4S (in ESI) and Table 4 give the steady-state NOE's and molecular modelling data, respectively, for the E isomer of **8**. The planar conformations of three major families generated by MMX are given in Scheme 2. NOE enhancements between C^2H and C^NH protons (19.1 and 22.9% in both directions) clearly indicate that conformation E–Z^t is the prevailing one. Averaging 5% of E–E^t (**1**) and 95% of E–Z^t (**3**) lowers the RMS to 0.233 but this result is not statistically meaningful. For the best conformation, (**3**), with an RMS of 0.240, the interval 0.19–0.329 defines the limits within which conformations cannot be distinguished as being different for a given precision of the NOE's. This means that conformations in Table 4, in bold, define equally well the mono-conformation model.

^3J(C,H) coupling constants. As pointed out above the NOE results for the group of C^1-alkyl-substituted β-sulfonyl enamines are not decisive as to whether the torsions C^1–N and N–C^N are conformationally homogeneous and recourse to proton-carbon couplings is the technique of choice in this case. For **8** Table 2S (see ESI) collects the necessary data required for the conformational analysis using this parameter. Compounds **3** and **4** give reference coupling constants with regard to the C^1–N torsion.

The conformations along the $\mathbf{C^2}$=C^1–N–**H** bond in enamines are of the Z–E type in the Z isomer of **3** and **4** and of the E–Z type in the E isomer of **3** (as established at −20 °C in equilibrium with the E–E conformation). The Z–E and E–Z conformers are characterised by $^3J(\mathbf{C^2}, N\mathbf{H})$ *ca.* 3.5 and 7 Hz, respectively. According to this, for compounds **8** and **9**, showing couplings of 6–6.5 Hz, the E–Z conformation is predicted.

The torsion along the N–C^N bond is probed by $^3J(\mathbf{C^1}, C^N\mathbf{H})$ and the complementary $^3J(N\mathbf{H}, C^N\mathbf{H})$ vicinal coupling constants. The former coupling is in the range of 2.2–3.9 Hz in both Z and E enamines with the smaller values being for the E isomer in all cases. This strongly suggests that the conformation along the inspected bond is of the transoid type in both enamines. The complementary vicinal proton-proton coupling constant $^3J(N\mathbf{H}, C^N\mathbf{H})$ has an expected value of *ca.* 13 Hz for the transoid disposition of protons (see above). However, in both enamine isomers this value is smaller, for example, 9 and 7.3 Hz for the Z and E forms of **8**, respectively. This can be treated as a hint that in both forms this bond is twisted to a different extent from the plane defined by H–N–C^N–H. In principle, the diminishing of the mentioned coupling constant, with respect to the predicted theoretical value, may indicate either a multi-conformation average or a distorted single conformation. Since the DNMR study does not show the presence of dynamic process down to −60 °C, the latter situation is more likely. Although chemical intuition would suggest a conformational manifold around this bond, one conformation, an E–Z^t type, is apparently prevailing.[20]

For the imine form of **8**, the E form is demonstrated by the observation of a NOE effect (17.8%) at C^NH upon irradiation of the C^1–CH_3 protons. An effect is also seen at the CH_2 resonance upon irradiation of the C^1–CH_3 protons (5.1%). NOE's are observed by irradiation of C^NH or CH_3 groups. For **7** the large NOE effect from the *t*-butyl group to the C^1H proton shows that the imine also has the E configuration.

Dynamics of tautomer exchange

Having elucidated the conformational equilibria the tautomeric equilibria of Scheme 1 can be discussed. The interconversion of E to I or Z forms may occur as (*i*) a unimolecular

process, (*ii*) in a dimer *via* a head-to-tail complex or (*iii*) in a process in which water is involved in all or some of the steps. With regard to (*ii*) the T_1 times for **8**, given in Table 1S (in ESI), do not indicate extensive long-lived dimer formation.

Kinetics of exchange. The slow exchange of tautomers on the NMR timescale at 500 MHz can be followed in 1D saturation transfer experiments or 2D ROESY spectra.[25] Compound **8** was chosen for saturation transfer experiments because of good signal separations and the presence of appreciable amounts of imine in $CDCl_3$ solution. In Scheme 3 the exchange between the three forms in equilibrium is exemplified by the data for the C^1–CH_3 methyl group and the C^NH proton.

The values of the saturation transfer in the 1D steady-state experiments are given in Table 5. Three sets of data were acquired, aimed at establishing the influence of water content and the solute concentration on the rate of exchange. This dependence is clearly seen on the I ⇋ Z equilibrium but not on the E ⇋ I equilibrium. In general, the former process is accelerated with an increase of water content in the sample (Scheme 3 and Table 5). Another important conclusion from these experiments is that the direct Z ⇋ E exchange is not observed under the studied conditions. Apparently, the amount of water present or the sample concentration do not play a role.

Rearrangement mechanism. The only mechanism studied so far is the sigmatropic rearrangement *in vacuo*.[8] The barrier for proton transfer is rather high.[8] Furthermore, the present conformational studies have shown that the E–E conformation is not easily obtained for some of the compounds. The X-ray study of **8**[24] (Table 4) showed an E–Z conformation in the solid state and this conformation is not suitable for the intramolecular 1,3-sigmatropic proton transfer. This conformation must also be present in solution immediately after the compound is dissolved in $CDCl_3$. In contrast to this, in compounds **6** and **7**, the E–E conformation is easily confirmed from the $^3J(C^1\mathbf{H},N\mathbf{H})$ value. From the DNMR results we also know that the E–E conformation is present in minor amounts in **1**–**4** (Table 1). The unsubstituted, **1**–**4**, and the C^1-substituted compounds, like **8**, thus show rather different conformational behaviour with respect to the E–E form. Nevertheless, as we have shown in the Results section, the saturation transfer experiments give rather similar results for **4** and **8** (compare Table 5S and Table 5, respectively). If one assumes, as discussed previously, that the E–E species may be present as a transient species in **8**, then only the energy profile along the C^1–N bonds determines its concentration. The *ab initio* calculations of the energy profile along the C^1–N bond show the latter conformation to be higher in energy by 2 kcal mol^{-1} with respect to the predominant E–Z conformation.[20] The E–E conformation seems to be involved in the rate-limiting step of the E ⇋ I equilibrium. The experimental results support this hypothesis: the independence of the rate of the E ⇋ I tautomerisation step on the solute and water content. In contrast, the I ⇋ Z step is shown in the same experiment to depend on the water content.

Based on the saturation transfer experiments discussed above, the involvement of water is very plausible in the I ⇋ Z tautomerisation step (Scheme 4). In Table 6 the saturation transfer experiment for the exchangeable protons are cited for **8**. The illustration of water involvement in a mechanism, supported by the data from Table 6, is given in Scheme 4.

Irradiation of the water resonance will result in a negative NOE at CH_2 of I, but not at the C^2H of E or Z as these are converted to I in the process. As neither E or Z transfer proton to water from their C^2 positions, irradiation of C^2H will not give rise to a negative NOE. If one irradiates the C^2H_2 of I, then, as one proton is transferred to water, one obtains a negative effect at water. Of primary importance is the fact that we do observe the reverse effect here, that is irradiation of water gives a negative effect on the imine C^2H_2 protons, but not on C^2H of E and Z. The most plausible explanation is the involvement of the enamine C^2 carbon, which is interacting with H_2O, as shown in Scheme 4. On the other hand, the saturation transfer data given in Table 6 can, in principle, be explained by assuming only simple exchange of N**H** protons of E and Z enamines and a direct exchange of the C^2H protons (anion mechanism) of the imine with water. However, the latter is highly unlikely at the used pH. Therefore, the above reasoning points to water involvement in the equilibria of tautomers as shown in Scheme 4.

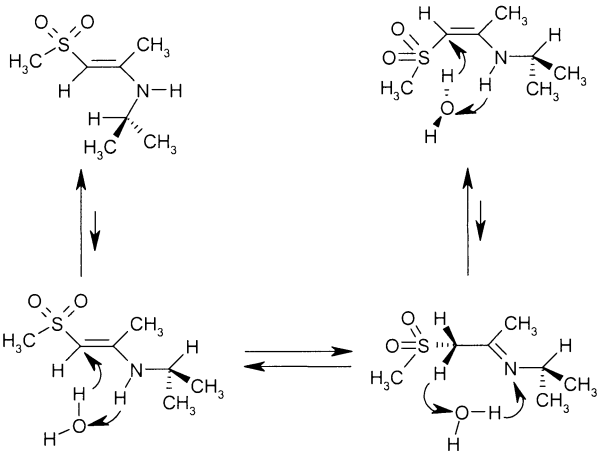

Scheme 4 Overview of suggested reaction mechanism. Arrows indicate the direction of proton transfer, not electron transfer. Free rotation around the C^2–C^1 bond in the imine enables one of the C^2H_2 protons to transfer to water, yielding E or Z enamines. The geometry of the imine is taken from the DFT calculations (Table 4).

E, Z and imine populations

The relative amounts of the enamines E or Z and imine may be discussed in a qualitative way. As pointed out previously, the enamine E and Z forms can be compared based on hydrogen bond and steric arguments. The hydrogen bond effects are not discussed in the present work as they require detailed interpretation of ^1H, ^{13}C, ^{15}N and ^{17}O data and are deferred to a later publication.[24]

The occurrence of the imine is more difficult to rationalize as this must be based on the relative stability compared with both the Z and E forms.

For the linear compounds **1**–**4** the E form becomes sterically more hindered the larger the N-substituent becomes. **1** and **2** are fully in the E–Z form, **4** is fully in the E–E form whereas **3** is a conformational mixture of these two. Compounds **1** and **2** are stabilised by an overlap between the CH_2 groups and the double bond.[26,27] The increasing steric interaction in **4** will thus lead to a destabilisation of the E form as seen by the comparison with **1**–**3**.

For the compounds with a methyl substituent at C^1, **8** and **9**, introduction of a large substituent on the nitrogen atom leads to severe steric interactions. For compounds **8**, with an *iso*-propyl substituent, and **9**, with a *t*-butyl substituent, the enamine E remains mainly in the E–Z form, probably less sterically hindered (*peri* type interaction between a C^2H and a CH_3 group, **B** in Scheme 5), in contrast to the enamine Z form (**C** in Scheme 5) and the imine I–E form (**D** in Scheme 5). This interaction clearly gives more steric hindrance as no E–E form with a similar motif (E–E^t, **A** in Scheme 5) is observed. This results in a relative destabilisation of the I–E and Z–E forms, in agreement with experimental observation, despite the fact that buttressing of the Z–E forms leads to stronger hydrogen bonding.

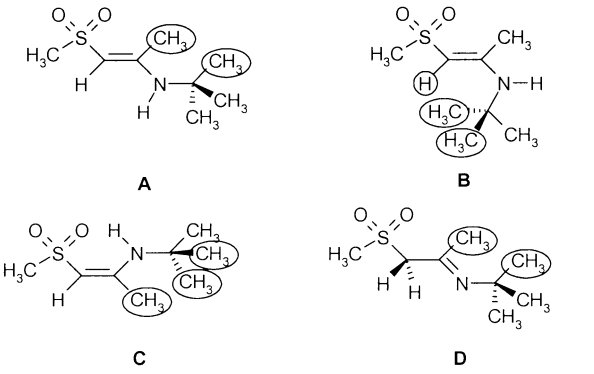

Scheme 5 Steric interactions in tautomeric forms of **9**.

In the C^2-substituted compound **6**, the imine is negligibly populated, most likely due to steric hindrance of C^2 by the methyl group. On the other hand, the cyclic compound **7** has the largest amount of imine found in the compounds studied. It can be suggested that this is mainly the effect of enhanced thermodynamic stability of the imine form, which is free of strain generated by the 5-membered ring and the exocyclic double bond in the enamine.

Conclusions

In this contribution we have presented a detailed study of the tautomeric composition and conformational space generated by all bonds in the parent aliphatic β-sulfonyl enamines having three types of double bond substitution. This was primarily achieved by the thorough analysis and interpretation of ^{1}H, ^{15}N NMR chemical shifts, NOE and ^nJ(H,H) or ^nJ(C,H) data and classical DNMR studies. Molecular modelling, on the MMX level and with the DFT approach, was used for the generation of the theoretical conformational space to compare with NOE experiments. Furthermore, we have established the involvement of the imine in the exchange process Z ⇋ E. This was achieved by studying the fate of the water protons in $CDCl_3$ solution in saturation transfer experiments in selected compounds, showing comparable populations of the three tautomeric forms in slow equilibrium.

It was found, in $CDCl_3$ solution, that the enamine E form predominates over the Z form in unsubstituted or acyclic β-methyl-substituted double bond compounds whereas the amount of imine is negligible. In β-substituted cyclic compounds, with an exocyclic double bond, the enamine E form exists in a slow equilibrium with imine. On the other hand the enamine Z form predominates in β-methyl-substituted compounds over the enamine E, with the E and imine forms present in comparable amounts. We have shown that in cyclic β-alkyl-substituted derivatives the amount of imine may reach *ca.* 60%. This is an important finding for applications in the synthesis of the studied class of compounds (see the introductory remarks).

The rotation around the S–C^2 bond is free in all acyclic compounds studied. The rotation around the C^1–N bond is hindered at *ca.* −20 °C in unsubstituted derivatives, but not in α-substituted derivatives. This gives rise to a conformational diversity in the three groups of studied compounds. On the other hand, a knowledge of the conformation around the C^1–N bond is important for theoretical *ab initio* calculations of imine-enamine tautomerisation, which require the E–E conformation for the intramolecular 1,3-sigmatropic NH proton transfer to the C^2 carbon atom. With respect to this we have found that in compounds **1**–**4**, unsubstituted on the double bond, there is a mixture of E–E and E–Z conformations that depends on the size of the substituent on the nitrogen atom. In the β-methyl-substituted compound **6** and cyclic β-alkyl-substituted **7** this conformation is E–E whereas in the β-methyl-substituted derivatives **8** and **9**, there is a preference for the E–Z conformations although the experimental approaches used in this work [NOE and ^3J(C,H); (H,H) coupling constants][20] do not allow for a rigorous exclusion of a small amount of E–E in the conformational equilibrium. Despite this diversity of stereochemistries around the C^1–N bond we do not observe a dramatic difference in the behaviour of the three groups of compounds in the saturation transfer experiments aimed at establishing the kinetics of NH proton transfer. This, in turn, may indicate a relative unimportance of the direct intramolecular NH proton transfer in the tautomerisation mechanism, at ambient temperatures in these compounds, if the E–E conformation is essential.

The saturation transfer experiments, performed in $CDCl_3$ solution, show that the mechanism of tautomerisation proceeds in two steps having probably different reaction orders. These are the E ⇋ I isomerisation and I ⇋ Z isomerisation, the rate of the former being independent of the solute and water concentration and the latter dependent on the presence of water. Under the studied conditions no direct Z ⇋ E isomerisation was observed in the saturation transfer experiments. Thus, for the first time, we have established in these experiments the intermediacy of the imine form in the Z ⇋ E isomerisation process in β-sulfur-substituted enamines, a long-lived presumption in enamine chemistry born out of chemical intuition. The intermolecular proton transfer *via* head-to-tail dimers of the E forms has been disregarded and the intramolecular 1,3-sigmatropic shift of the NH proton considered as a potential mechanism characterised by a higher energy transition state.

Experimental

Synthesis

The synthesis of all compounds and analysis of the MS spectra is prepared for publication.[28] The compounds were synthesised applying modified procedures of published methods or new procedures for this class of compounds.[29]Compounds **1**–**4** were synthesised in a one-pot reaction by action of NaH on dimethyl sulfone and ethyl formate addition in diethyl ether and subsequent condensation of the formed sodium enolate with amine hydrochlorides. Compound **5** was synthesised using the procedures applied for compounds **1**–**4**. Compounds **6** and **7** were synthesised by generating the enolates as above, using *n*-BuLi, from the appropriate sulfones, that is diethyl sulfone and 1,1-dioxo-1-thiacyclopentane, respectively, isolation and their reaction with amine hydrochlorides. Compounds **8** and **9** were synthesised by condensation of the sulfone with an excess of amine in boiling benzene, in the presence of *p*-toluene sulfonic acid and a drying agent, by analogy to a method used for β-ketoenamines,[30] applied to β-sulfonyl enamines.[31] All compounds studied were characterised satisfactorily using IR, elemental analyses and MS spectroscopy. They were crystallised from methanol and melted within 2 °C.

Characterization of compounds 1–9. 1. Anal. calcd for $C_4H_9NSO_2$: C, 35.54; H, 6.71; N, 10.36; S, 23.72; found: C, 35.03; H, 6.60; N, 10.28; S, 23.60. MS (EI): *m*/*z* 135.1 (58). IR (KBr): *v* 3363.8, 3077.3, 3007.7, 2928.3, 2904.8, 1631.2, 1314.0, 1108.0 cm^{-1}.

2. Anal. calcd for $C_5H_{11}NSO_2$: C, 40.42; H, 7.41; N, 9.36; S, 21.38; found: C, 40.13; H, 7.55; N, 9.42; S, 21.28. MS (EI): *m*/*z* 149.1 (67). IR (KBr): *v* 3348.0, 3074.6, 3017.0, 2982.3, 2931.3, 2900.2, 1622.7, 1323.5, 1105.3 cm^{-1}.

3. Anal calcd for $C_6H_{13}NO_2S$: C, 44.15; H, 8.03; N, 8.58; S, 19.64; found: C, 44.26; H, 7.95; N, 8.52; S, 19,77. MS (EI): *m*/*z*

163.0 (37). IR (KBr): ν 3339.1, 3045.2, 2971.4, 2926.7, 2874.0, 1618.6, 1322.8, 1111.6 cm^{-1}.

4. Anal. calcd for $C_7H_{15}NO_2S$: C, 47.43; H, 8.53; N, 7.90; S, 18.09; found: C, 47.21; H, 8.33; N, 7.67; S, 18.16. HR-MS: m/z 177.08221 (calcd 177.0824). IR (KBr): ν 3324.8, 3065.7, 2968.2, 1637.7, 1487.8, 1370.9, 1257.0, 1108.6, 972.6, 857.9, 779.5, 745.3, 533.3, 513.0 cm^{-1}.

5. Anal calcd for $C_7H_{13}NO_3S$: C, 43.96; H, 6.85; N, 7.32; S, 16.76; found: C, 43.95; H, 7.05; N, 7.39; S, 16.63. MS (EI): m/z 191.2 (67). IR (KBr): ν 3074.0, 3010.4, 2986.4, 2925.3, 2862.7, 1624.9, 1318.6, 1118.4 cm^{-1}.

6. HR-SIMS: m/z 205.2 (calcd for $C_9H_{19}NO_2S$: 205.1137). IR (KBr): ν 3351.6, 2965.8, 2931.7, 1643.6, 1259.0, 1095.05 cm^{-1}. ^{13}C NMR (45 mg in 0.7 mL $CDCl_3$) enamine E: δ 7.58 [CH_3–C–S, $^1J = 129.8$, $^3J(CH_2) = 5.5$ Hz], 9.42 [C^2–CH_3, $^1J = 128.4$, $^3J(C^1H) = 5.5$ Hz], 30.17 [N–C–$(CH_3)_3$, $^1J = 125.6$, $^3J(NH) = 2.0$, $^3J(CH_3) = 47.46$ Hz, S-CH_2, $^1J = 135.9$, $^3J = 4.5$ Hz], 51.95 (N–C^N), 97.05 [C^2, $^2J(CH_3) = 6.2$, $J = 2.7$ Hz (not assigned to NH or C^1H)], 141.82 [C^1, $^1J = 167.0$, $^3J(CH_3) = 3.8$ Hz].

7. Anal. calcd for $C_9H_{16}NO_2S$: C, 53.17; H, 8.43; N, 6.89; S, 15.77; found: C, 53.30; H, 8.62; N, 7.05; S, 5.65. HR-MS: m/z 203.0986 (calcd for $C_9H_{16}NO_2S$: 203.0980). IR (KBr): ν 3333.6, 2965.8, 1658.8, 1258.6, 1123.9 cm^{-1}.

8. HR-MS: m/z 177.081 (calcd for $C_7H_{15}NO_2S$: 177.0823). IR (KBr): ν 3316.2, 3073.8, 2974.7, 2933.9, 1586.3, 1315.8, 1098.4 cm^{-1}.

9. HR-MS: m/z 191.0986 (calcd for $C_8H_{17}NO_2S = M^+$: 191.0980). IR (KBr): ν 3315.5, 2997.7, 2941.6, 1307.8, 1105.2 cm^{-1}. ^{13}C NMR (120 mg in 0.7 mL $CDCl_3$) enamine E/Z: δ 18.75/20.69 (C^1–CH_3), 27.81/30.50 [N–C^N–$CH_3)_3$], 45.42/44.20 (S–CH_3), 51.13/51.83 (N–C^N), 92.27/88.27 (C^2), 153.92/157.19 (C^1).

NMR

The gradient ^1H-^{13}C HMBC[32] spectra were obtained on a Varian INOVA 500 spectrometer operating at 499.806 MHz for ^1H observation. The data were acquired as a 2048×1024 matrix processed in absolute value mode in F_1 with 64 transients per t_1 increment. The ^nJ(C,H) was optimised for 8 Hz and low-pass filter for ^1J(C,H) = 140 Hz. The data were linear-predicted to 2048 points and zero-filled to 4096 points in F_1 prior to Fourier transformation.

The gradient ^1H-^{13}C HSQC,[33] one-bond correlation spectra, were run in the relevant acquisition and processing conditions.

The ^1H-^{15}N HMQC spectra were recorded with a spectral width of 5000 Hz, 2048 points in the ^1H dimension and 19226 Hz in the ^{15}N dimension, 256 increments, ^nJ(N,H) = 4.5 Hz; 96 transients were recorded for each increment, with a relaxation delay of 1 s. ^1H-^{15}N HSQC were run in the same conditions, using ^1J(N,H) = 90 Hz and 4096 data points in the ^1H dimension to afford better resolution when reading the ^nJ(H, N) coupling constants in F_2.

T_1 relaxation times were measured using standard Varian software using 25 s as the recovery time in the sequence.

The samples for NOE studies and saturation transfer experiments (5 mg in 0.7 mL of $CDCl_3$) were prepared using standard freeze-thaw techniques and stored under argon. The NOE experiments were run at $-15\,^\circ C$ to avoid the effects of saturation transfer in an equilibrating system. The experimental error indicated in Tables 3S and 4S on the C^1 methyl group may arise from the different rotational correlation time for the methyl with respect to the whole molecule. This effect is not explicitly treated in the NOE program [23] and may cause the observed discrepancies in experimental and calculated values.

The saturation transfer experiments were run on the equilibrated samples with the same concentrations as used for the NOE measurements and using the same program for saturating the multiplets. The experimental conditions for both types of experiments were as follows: 5000 Hz spectral window and 64K points, 15 s irradiation time and 2 s acquisition time. The spectra were analysed in absorption mode using the same phase parameters for the reference and irradiated spectra.

Molecular modelling

The search for low energy conformers was carried out by systematic conformational searching using the PCMODEL[34] program employing the MMX force field. Gas-phase geometries of selected conformers were optimised at the HF 6-31G** and BLYP/6-31G** levels using the TURBOMOL[35] program.

Acknowledgements

This work was supported by the Drug Institute and the Institute of Organic Chemistry Polish Academy of Sciences. WK thanks the Warsaw University for a grant No. 120-501/68/BW-1483/14/2000.

References

1 G. Lombardino, *Nonsteroidal Antiinflammatory Drugs*, Wiley Intersciences, J. Wiley & Sons, New York, 1985.
2 (*a*) *The Chemistry of Sulfones and Sulfoxides*, ed. S. Patai, Z. Rappoport and C. J. M. Stirling, J. Wiley, New York, 1988; (*b*) *Syntheses of Sulfones, Sulfoxides and Cyclic Sulfides*, ed. S. Patai and Z. Rappoport, J. Wiley, New York, 1994.
3 E. Block, *Reactions of Organosulfur Compounds*, Academic Press, New York, 1978.
4 A. Arnone, P. Bravo, S. Capelli, G. Fronza, S. V. Meille and M. Zanda, *J. Org. Chem.*, 1996, **61**, 3375.
5 *The Chemistry of Enols*, ed. Z. Rappoport, J. Wiley, Chichester, 1990.
6 J. Toullec, *Adv. Phys. Org. Chem.*, 1982, **18**, 1.
7 K. Lammerstma and B. V. Prasad, *J. Am. Chem. Soc.*, 1994, **116**, 642.
8 C.-C. Su, C.-K. Lin, C.-C. Wu and M.-H. Lien, *J. Phys. Chem. A*, 1999, **103**, 3289.
9 J.-F. Ling, C.-C. Wu and M.-H. Lien, *J. Phys. Chem.*, 1995, **99**, 16903.
10 R. A. Poirier and D. Majlessi, *J. Comput. Chem.*, 1986, **7**, 4464.
11 C. H. McMullen and C. J. M. Stirling, *J. Chem. Soc. B.*, 1966, 1217.
12 Y. Kurasawa, A. Takeda and H. S. Kim, *Heterocycles*, 1995, **41**, 2057.
13 J. E. Douglass and M. A. Gebhart, *J. Heterocycl. Chem.*, 1990, **27**, 1433.
14 S. Kobayashi and H. Ishitani, *Chem. Rev.*, 1999, **99**, 1069.
15 S. E. Denmark and O. J.-C. Nicaise, *Chem. Commun.*, 1996, 999.
16 L. Kozerski, R. Kawęcki, P. Krajewski, B. Kwiecień, D. W. Boykin, S. Bolvig and P. E. Hansen, *Magn. Reson. Chem.*, 1998, **36**, 921.
17 L. Kozerski, R. Kawęcki and P. E. Hansen, *Magn. Reson. Chem.*, 1994, **32**, 517.
18 M. Witanowski, L. Stefaniak and G. A. Webb, *Annu. Rep. NMR Spectrosc.*, 1993, **25**, 1.
19 W. Koźmiński and D. Nanz, *J. Magn. Reson.*, 2000, **142**, 294.
20 W. Koźmiński, E. Bednarek, W. Bocian, J. Sitkowski, P. E. Hansen, B. Kwiecień and L. Kozerski, *Magn. Reson. Chem.*, 2000, **38**, 839.
21 E. Osawa, T. Ouchi, N. Saito, M. Yamato, O. S. Lee and M.-K. Seo, *Magn. Reson. Chem.*, 1992, **30**, 1104.
22 L. Kozerski, R. Kawęcki, P. Krajewski, P. Gluziński, K. Pupek, P. E. Hansen and M. P. Williamson, *J. Org. Chem.*, 1995, **60**, 3533.
23 L. Kozerski, P. Krajewski, K. Pupek, P. G. Blackwell and M. P. Williamson, *J. Chem. Soc., Perkin Trans. 2*, 1997, 1811.
24 L. Kozerski, B. Kwiecień, R. Kawęcki, E. Bednarek, W. Bocian, J. Sitkowski and P. E. Hansen, *J. Crystallogr. Spectrosc. Res.*, unpublished results.
25 A. Bothner-By, L. H. Stephens, I. Lee, C. Warren and R. Jeanloz, *J. Am. Chem. Soc.*, 1984, **106**, 811.
26 N. J. Koole, M. J. A. de Bie and P. E. Hansen, *Org. Magn. Reson.*, 1984, **22**, 146.

27 F. Bernardi, N. D. Epiotis, R. L. Yates and H. B. Schlegel, *J. Am. Chem. Soc.*, 1976, **98**, 2385.
28 L. Kozerski, B. Kwiecień, R. Kawęcki and J. Witowska, unpublished results.
29 B. Kwiecień, Ph.D. Thesis, Institute of Organic Chemistry, Polish Academy of Sciences, Warszawa, 2000.
30 P. W. Hickmott, *Tetrahedron*, 1982, **38**, 3363.
31 S. Fatutta, G. Pitacco and E. Valentin, *J. Chem. Soc., Perkin Trans. 1*, 1982, 2045.
32 A. Bax and M. F. J. Summers, *J. Am. Chem. Soc.*, 1986, **108**, 2093.
33 M. F. J. Summers, L. G. Marzili and A. Bax, *J. Am. Chem. Soc.*, 1986, **108**, 4285.
34 PCMODEL, Molecular Modelling Software, Serena Software, Bloomington, IN, USA.
35 R. Ahlrichs, M. Bär, M. Häser, H. Horn and C. Kölmel, *Chem. Phys. Lett.*, 1989, **162**, 165.